

Baitak Apshikur<sup>1</sup>, Elibek A. Asangaliyev<sup>2</sup>, Murat A. Rakhimov<sup>3</sup>, Elena V. Medvedeva<sup>4</sup>

## INTEGRATION OF RS DATA AND UAV DATA FOR AGRICULTURAL PRODUCTIVITY ASSESSMENT AND DIFFERENTIAL FERTILIZATION IN KAZAKHSTAN

### ABSTRACT

This study explores the use of Unmanned Aerial Vehicles “UAVs” and Remote Sensing “RS” data to assess the productivity of agricultural lands in various regions of Kazakhstan. The primary focus is on analyzing vegetation indicators such as the Normalized Difference Vegetation Index “NDVI” and their relationship with the agrochemical properties of the soil. A comparative analysis was performed between satellite multispectral imaging and UAV-based aerial photography to determine the most accurate methods for predicting spring barley yield. The integration of RS technologies with traditional agricultural methods has proven to reduce environmental impact, minimize soil degradation, and enhance the stability of agroecosystems. Field experiments took place in three different soil-climatic zones of Kazakhstan, with spring barley cultivated under controlled conditions. The study included multispectral imaging from Landsat-8–9 satellites and UAV-based multispectral imaging. The results indicate that differentiated fertilization strategies, based on the spatial distribution of soil nutrients, contribute to increased crop productivity and reduced excessive nitrogen application. The findings of this study highlight that the implementation of precision agricultural technologies can significantly improve yield prediction accuracy and resource efficiency. Moreover, integrating UAV-based monitoring with GIS mapping enables real-time decision-making in farm management. These approaches promote sustainable agricultural practices by reducing soil degradation and enhancing long-term productivity through environmentally friendly farming methods. The results of this study are applicable to the development of sustainable agricultural strategies aimed at enhancing productivity while conserving natural resources, thereby ensuring long-term food security and environmental stability.

**KEYWORDS:** yield prediction, satellite multispectral image, field scale, barley, vegetation index

### INTRODUCTION

With the advancement of remote sensing and satellite monitoring technologies, and the growing availability of satellite imagery worldwide, precision agriculture systems are increasingly being adopted in agricultural practices [Toguzova et al., 2022]. The main goal of precision agriculture in crop production is to maximize productivity and financial returns while minimizing costs and environmental impact [Beluhova-Uzunova, Dunchev, 2019]. Its scientific foundation is based on the concept of intra-field variability [Kulyasov et al., 2020]. Heterogeneous soil layers within cultivated fields can lead to inconsistent yield potential under uniform management. Identifying such areas

<sup>1</sup> D. Serikbayev East Kazakhstan Technical University, School of Earth Sciences, 69, Protozanova str., Ust-Kamenogorsk, 070004, Kazakhstan, e-mail: [bapshikur@edu.ektu.kz](mailto:bapshikur@edu.ektu.kz)

<sup>2</sup> D. Serikbayev East Kazakhstan Technical University, School of Earth Sciences, 69, Protozanova str., Ust-Kamenogorsk, 070004, Kazakhstan, e-mail: [elibek60@mail.ru](mailto:elibek60@mail.ru)

<sup>3</sup> Abylkas Saginov Karaganda Technical University, Department of Building Materials and Technology, 56, Nursultana Nazarbayeva ave., Karaganda, 100027, Kazakhstan, e-mail: [rahimov67@mail.ru](mailto:rahimov67@mail.ru)

<sup>4</sup> D. Serikbayev East Kazakhstan Technical University, School of Earth Sciences, 69, Protozanova str., Ust-Kamenogorsk, 070004, Kazakhstan, e-mail: [emedvedeva@edu.ektu.kz](mailto:emedvedeva@edu.ektu.kz)

enables reduced treatment zones, optimized fertilizer use, and lower average production costs, while improving overall productivity [Korchagin et al., 2021; Apshikur et al., 2024].

Currently, the application of precision agriculture methods in the agricultural sector serves as one of the key approaches for increasing productivity, optimizing resource use, and assessing the level of geoecological contamination in cultivated lands within industrial regions, such as the areas studied in this research [Apshikur et al., 2024]. Furthermore, these methods play a crucial role in planning measures to mitigate such contamination. Precision agriculture integrates modern technologies in crop production, including Remote Sensing and the use of Unmanned Aerial Vehicles “UAVs” [Cao et al., 2023]. Compared to ground-based and satellite monitoring methods, UAV-derived data are distinguished by higher accuracy, enabling rapid assessment of the condition of agricultural fields [Phang et al., 2023].

Currently, remote sensing “RS” data are being increasingly utilized in various critical sectors of the national economy, including the monitoring of vegetation cycles across vast agricultural territories [Erunova et al., 2021], early prediction of forest fires [Asangaliyev et al., 2024], forecasting flood risks and assessing their consequences [Apshikur et al., 2023], evaluating the environmental impact of waste dumps from mineral extraction and delineating their spread [Ryzhkov et al., 2021], as well as optimizing urban traffic management and obtaining real-time information on traffic congestion [Abedzhanova et al., 2023]. Moreover, in emergency situations, data obtained from various types of “UAVs” are increasingly being integrated into these applications.

The increasing number of orbiting satellites, along with their multifunctional spectral channels (e. g., the Landsat-8–9 OLI-TIRS and Sentinel-1–2 series), provides valuable real-time satellite data. The availability of open-access satellite archives facilitates effective agricultural management. Moreover, these data enable the identification of chemical pollutants leaching from agricultural fields along riverbanks into water bodies. They also support the development of mitigation strategies [Apshikur et al., 2025]. In developed European countries, new approaches and strategies based on remote sensing techniques from ground-based, aerial, and satellite platforms for detecting weed infestations are widely implemented [Huang et al., 2018].

Aerial and space borne platforms serve as primary tools for acquiring “RS” data in addressing environmental and agricultural challenges. However, such data sources have several significant limitations. The most critical among them include the high cost of imagery, the restricted ability to obtain images within short timeframes and at the required frequency, the necessity for image interpretation, and errors induced by weather conditions, cloud cover, and fog.

Over the past decade, research on the use of drones in precision agriculture has increased tenfold. Today, various types of Unmanned Aerial Vehicles play a crucial role in providing high-quality remote sensing data at the necessary scale and within the required timeframe, effectively addressing the need for rapid and localized information acquisition [Jindo et al., 2021].

This study aims to evaluate the accuracy of methods utilizing UAV and remote sensing (RS) data for assessing crop productivity in agricultural lands across different regions of Kazakhstan. The primary objective is to determine the effectiveness of precision agriculture technologies by integrating satellite imagery, UAV-based high-resolution data, and geospatial tools for crop yield monitoring and management.

In the context of this study, the term “agricultural productivity assessment” refers to the evaluation of vegetation condition and potential yield using remote sensing-derived vegetation indices, primarily the Normalized Difference Vegetation Index (NDVI). NDVI served as a proxy for biomass density, photosynthetic activity, and crop health throughout the growing season. Productivity was assessed spatially by overlaying NDVI maps with interpolated soil nutrient data to identify low-performing zones and inform differential fertilizer application.

The study also aims to delineate the spatial boundaries of soil degradation using automated soil sampling, optimize variable-rate fertilization, and implement yield mapping techniques. Various vegetation indices, such as NDVI, EVI, and GNDVI [Jinru et al., 2017], were analyzed for their correlation with crop yield indicators. The advantages and limitations of each method were evaluated based on experimental data and high-resolution imagery obtained from both UAV and satellite platforms.

The research findings presented in this article result from the work conducted by the team of authors within the framework of the Scientific and Technical Program and Targeted Funding Project of the Ministry of Agriculture of the Republic of Kazakhstan for 2020–2023.

The results of the study contribute to the advancement of remote monitoring techniques in agriculture [Lebrini et al., 2020], enabling farmers and agronomists to make accurate and effective decisions. Furthermore, the obtained data highlight the importance of integrating digital technologies into the agricultural sector and support the future development of precision farming systems.

## RESEARCH MATERIALS AND METHODS

As the subject of the study, the cultivation of spring barley was examined in three regions of Kazakhstan's agricultural lands. Spring barley has a relatively short active period for nutrient uptake from the soil [Sadenova et al., 2022]. According to statistical calculations, the production of 1 ton of grain requires approximately 30 kg of nitrogen, up to 10 kg of phosphorus, and more than 27 kg of potassium. Therefore, fertilizers play a crucial role in enhancing plant growth and yield, as well as in preventing the natural depletion of soil resources.

Ground-based monitoring experiments were conducted at selected test sites, including Field 1 of Farm E, Field 2 of Farm N, and Field 3 of Farm M (Fig. 1).

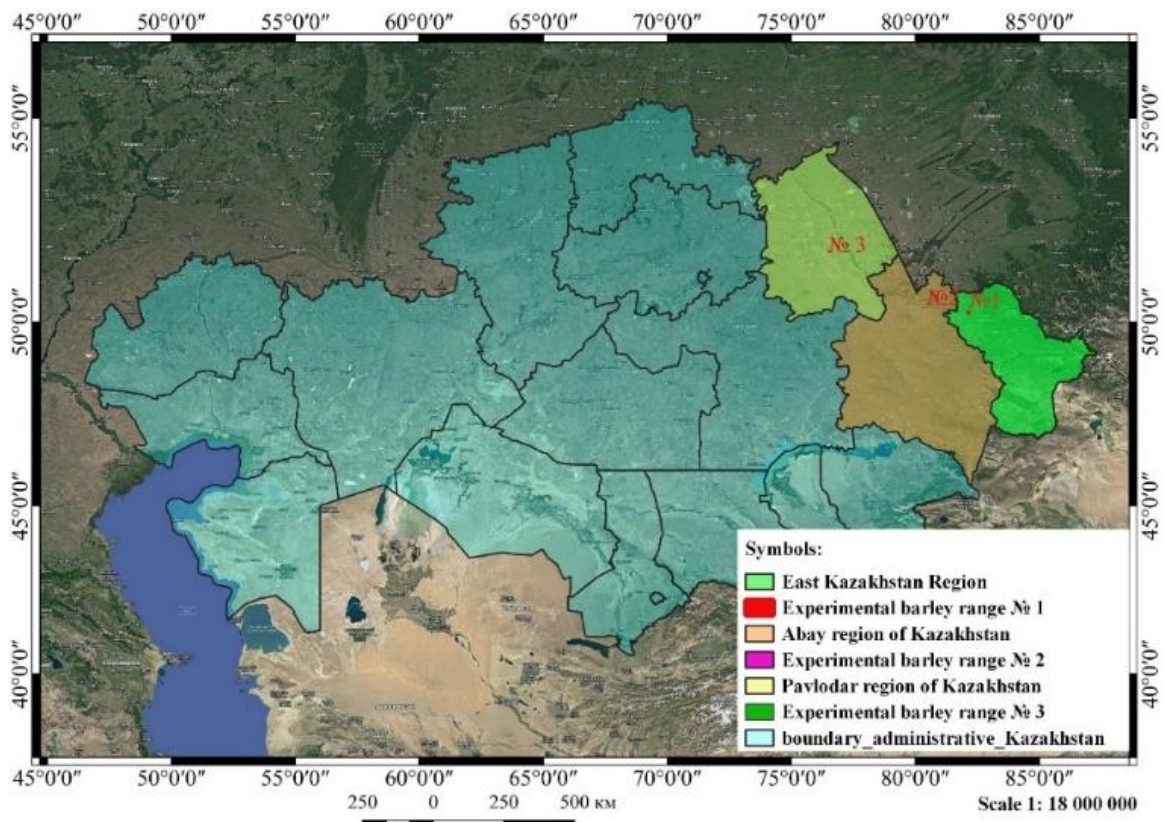


Fig. 1. Administrative division of Kazakhstan and the location of experimental sites (No. 1–3)

The studied fields for spring barley cultivation are located in different zonal regions and fall into distinct belt-specific categories.

Each field (Polygon 1–3) has an approximate area of 45 ha. These measurements were obtained using GPS-based field boundary mapping and confirmed using spatial analysis tools in QGIS, ensuring accuracy for further agrochemical mapping and UAV flight planning.

In general, Polygons 1–2 are located in a dry steppe zone and feature black and dark chestnut soils. In contrast, Polygon 3 comprises deep carbonate, weakly humus sandy and loamy sandy chestnut soils, as well as underdeveloped chestnut soils [Yapiyev et al., 2018].

The research process began with monitoring the spring fieldwork conducted in each polygon. For Polygon 1, spring barley seeds of the Elek-16 variety were sown in the first decade of May 2022 at an average seeding rate of 180 kg/ha and harvested at the end of July 2022 with a yield of 17.0 c/ha [Górski et al., 2023]. No mineral fertilizers were applied to the soil in the study area. Spring barley crops were treated with herbicides against weeds and pests [Bakaeva et al., 2024].

In Polygon 2, spring barley seeds of the Elek-16 variety were sown in the first decade of May 2022 at an average seeding rate of 180 kg/ ha and harvested at the end of August 2022 with a yield of 6.0 c/ha. No mineral fertilizers were applied to the study area.

Farmers applied herbicides to spring barley crops to control weeds and pests. In Polygon 3, farmers sowed spring barley seeds of the “Belcanta” variety in the first decade of May 2022 at an average seeding rate of 180 kg/ ha and harvested them at the end of August 2022, with a yield of 9 c/ha.

The study area involved the application of both primary and specialized mineral fertilizers [Deikun et al., 2022]. “Nitroammophoska” served as the primary fertilizer at a dosage of 250 kg/ha. Farmers applied herbicides to spring barley crops to control weeds and pests [Vlasenko et al., 2011].

During soil sampling, it was necessary to take into account various factors such as non-uniform soil cover, terrain features, climatic conditions, and vertical zonal structure. To analyze the agrochemical composition of soil fertility, researchers collected samples from the arable layer at a depth of 0–0.30 m [Yang et al., 2022].

The initial stage of the field study involved the creation of a high-precision digital field contour (map) using a GPS receiver (Fig. 2a). The GPS data collected from the field boundaries were imported into QGIS software (v. 3.38.0), where vector shapefiles were generated. These shapefiles served as base maps for further spatial analysis and mapping. Agrochemical maps were developed by interpolating laboratory soil test results (humus, nitrogen, potassium, phosphorus) using the Inverse Distance Weighting (IDW) method in QGIS, providing spatial distribution of soil nutrients across the plots. Following this, the plowing area was divided into ten 100 m<sup>2</sup> squares using a specialized tablet equipped with the Exact Farm application (Fig. 2b). Researchers designated the center of each square as a sampling point for soil collection [Huuskonen, Oksanen, 2018; Gonçalves et al., 2021]. Researchers collected soil samples from the designated locations determined by the GPS-enabled tablet using the “WINTEX 1000S” soil sampler, which can be attached to any agricultural machinery (Fig. 2c). The key advantage of this method is that the coordinates of each sampling point are stored in the tablet, enhancing the reliability of statistical data on soil changes in subsequent years after fertilizer application.

Composite soil samples were collected from experimental plots using the diagonal “envelope” method. Each composite consisted of 10 subsamples per plot. The samples were analyzed in the accredited “Veritas” laboratory at D. Serikbayev East Kazakhstan Technical University.

Based on the lab results, agrochemical maps were generated in QGIS, reflecting key soil parameters such as humus, exchangeable nitrogen, potassium oxide (K<sub>2</sub>O), sodium (Na), calcium (Ca), phosphorus pentoxide (P<sub>2</sub>O<sub>5</sub>), and others [Hoffland et al., 2020].

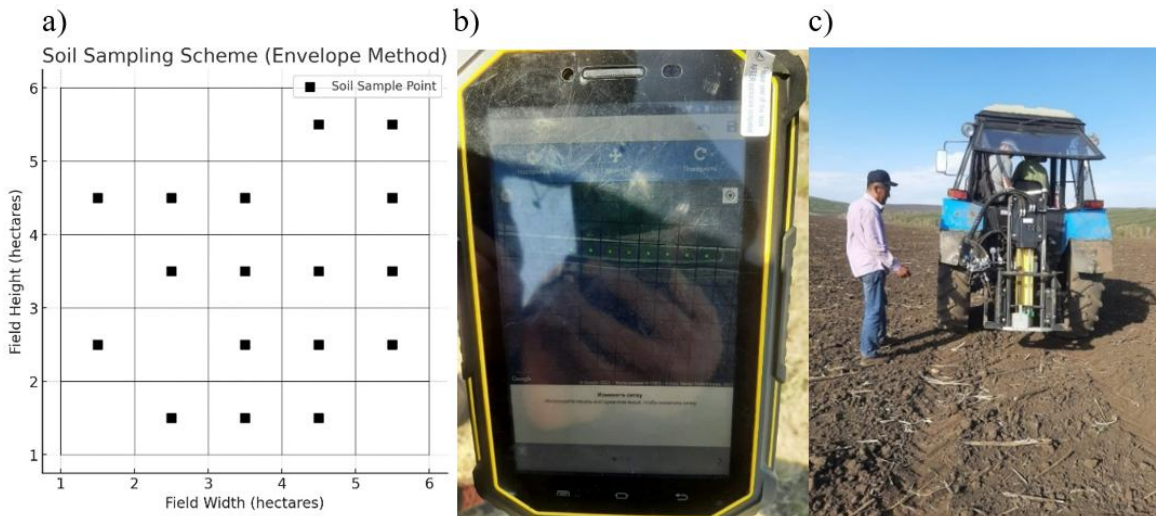


Fig. 2. Soil sampling in the polygon fields: (a) sampling methods, (b) GPS tablet, (c) Wintex 1000S soil sampler

Productivity indices were also determined for each vegetation period using satellite imagery (Landsat 8–9 OLI/TIRS, Sentinel-2). To validate these data, aerial surveys were carried out using the DJI Phantom 4 Multispectral UAV with D-RTK2 for precision agriculture (Fig. 3a).

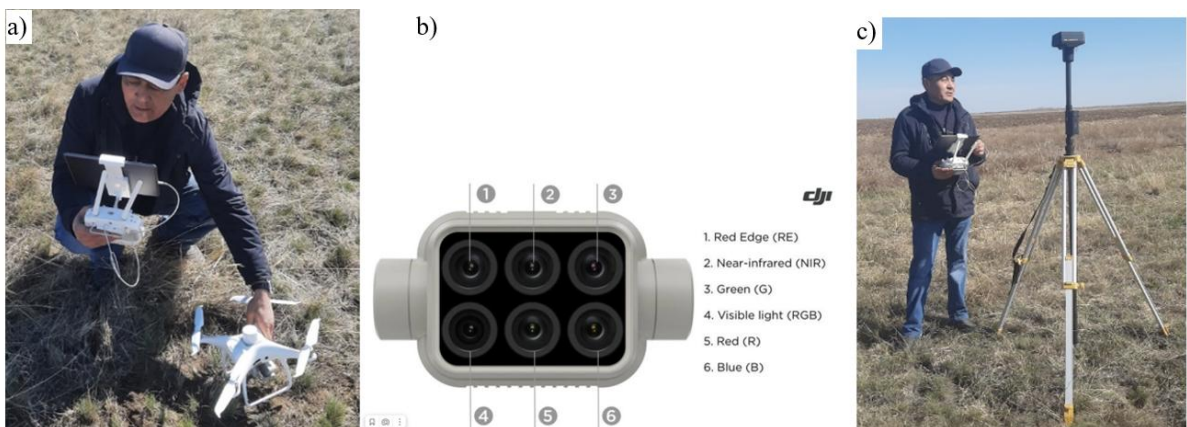


Fig. 3. Unmanned aerial vehicle (UAV) system: a) DJI Phantom and preparation process; b) multispectral camera; c) mobile station D-RTK2

The DJI Phantom 4 Multispectral “P4M” is a compact quadcopter designed for aerial multispectral imaging (Fig. 3b). It is an ideal solution for agricultural applications and comes equipped with the D-RTK 2 High Precision GNSS mobile station. The camera is equipped with six sensors, each capturing different spectral dimensions (Fig. 3c).

Multispectral images are processed using specialized agricultural software that extracts critical data in our case, “Agisoft Metashape”.<sup>1</sup> Agisoft LLC, headquartered in St. Petersburg, Russia, developed the software. This technology enables the generation of geospatial telemetry, soil, and crop data, allowing producers to efficiently manage and plan farm operations. It facilitates cost and time saving while optimizing resource use, reducing pesticide application, and enhancing overall farm management.

<sup>1</sup> Agisoft LLC. Wikipedia. Web resource: [https://en.wikipedia.org/wiki/Agisoft\\_LLC](https://en.wikipedia.org/wiki/Agisoft_LLC) (accessed 20.02.2025)

As outlined above, researchers analyzed satellite data for each vegetation period and captured UAV imagery to determine yield assessment indices after implementing yield improvement measures in cultivated fields. Vegetation indices are composed of reflectance measurements at two or more wavelengths to analyze specific plant characteristics, such as total leaf area and water content. More than 150 vegetation indices have been published in the scientific literature<sup>1</sup>, however, only a small number of them have a significant biophysical foundation or have undergone systematic validation. The most widely used vegetation index is NDVI “Normalized Difference Vegetation Index”, while NDRE “Normalized Difference Red Edge” is also frequently used, especially since detection with a Sentera sensor equipped with an additional NDRE filter provides more comprehensive data [Boiarskii, Hasegawa, 2019].

## RESEARCH RESULTS AND DISCUSSION

To determine the agrochemical properties of the soil and calculate fertilizer application rates, an agrochemical study was performed on the soil of experimental plots 1–3, considering the current years chemical analysis data on the mobile forms of nutrients [Surinov, 2023]. The primary components of soil fertility were determined in the three studied polygons (Table 1).

The analysis included humus content (percentage), soil acidity (pH), total sulfur (S total, %), and mobile sulfur (S mobile, mg/kg). Additionally, total nitrogen (N total, %), total nitrogen content (N total, mg/kg), and total nitrogen per 100 g of soil (N total, mg/100 g of soil) were measured. The study also determined mobile potassium (K<sub>2</sub>O, mg/kg), mobile potassium per 100 g of soil (K<sub>2</sub>O, mg/100 g of soil), mobile phosphorus (P<sub>2</sub>O<sub>5</sub>, mg/kg), and mobile phosphorus per 100 g of soil (P<sub>2</sub>O<sub>5</sub>, mg/100 g of soil). Furthermore, heavy metal concentrations were assessed, including lead (Pb, mg/kg), iron (Fe, mg/kg), copper (Cu, mg/kg), zinc (Zn, mg/kg), nickel (Ni, mg/kg), manganese (Mn, mg/kg), calcium (Ca, mg/kg), magnesium (Mg, mg/kg), and chromium (Cr, mg/kg) [Muraru et al., 2021]. The key indicators constituting the main components of soil fertility were determined separately for each of the three studied polygons.

Based on the research results, agrochemical maps displaying the levels of mobile nutrients were prepared. Considering the publications space limitations, this article presents fragments of the maps for Polygon 1 (Fig. 4).

Based on the results of the agrochemical analysis, the humus content in the examined plots of Polygon 1 the study determined to range from 4.06 to 5.32 %, indicating that the soil is rich in organic matter. The pH level of the soil solution varied between 6.68 and 8.04, spanning from slightly acidic to mildly alkaline conditions. The total nitrogen (N total) content ranged from 2 156 to 3 108 mg/kg, while the total nitrogen content per 100 g of soil varied from 215.6 to 310.8 mg/100 g, suggesting that the studied soils contain a sufficient amount of nitrogen. The concentration of mobile phosphorus (P<sub>2</sub>O<sub>5</sub>) ranged from 54.40 to 66.80 mg/kg, whereas the mobile potassium (K<sub>2</sub>O) content was determined to be between 354 and 396 mg/kg. The phosphorus content per 100 g of soil the study determined to range from 5.44 to 6.68 mg/100 g, while the potassium content varied between 35.4 and 39.6 mg/100g [Lukin, 2017].

These data indicate that the studied soils are moderately to highly supplied with potassium and phosphorus. Based on the high natural humus content in the soil, the conducted studies estimated that, considering the additional yield, the nutrient uptake by crops in the current year, under favorable weather and climatic conditions, allows for obtaining 17.0 c/ha of spring barley yield.

Similarly, according to the agrochemical analysis results, the humus content in the soil of Polygon 2 the study determined to range from 3.50 to 5.50 %. The pH value of the soil solution varied between 5.59 and 7.51, indicating a reaction from slightly acidic to neutral. The total

<sup>1</sup> Vegetation index. Wikipedia. Web resource: [https://en.wikipedia.org/wiki/Vegetation\\_index](https://en.wikipedia.org/wiki/Vegetation_index) (accessed 01.03.2025)

nitrogen (N total) content ranged from 2 044 to 2 772 mg/kg, suggesting that the studied soils contain a sufficient amount of nitrogen.

*Table 1. Laboratory Agrochemical Indicators of the Soil*

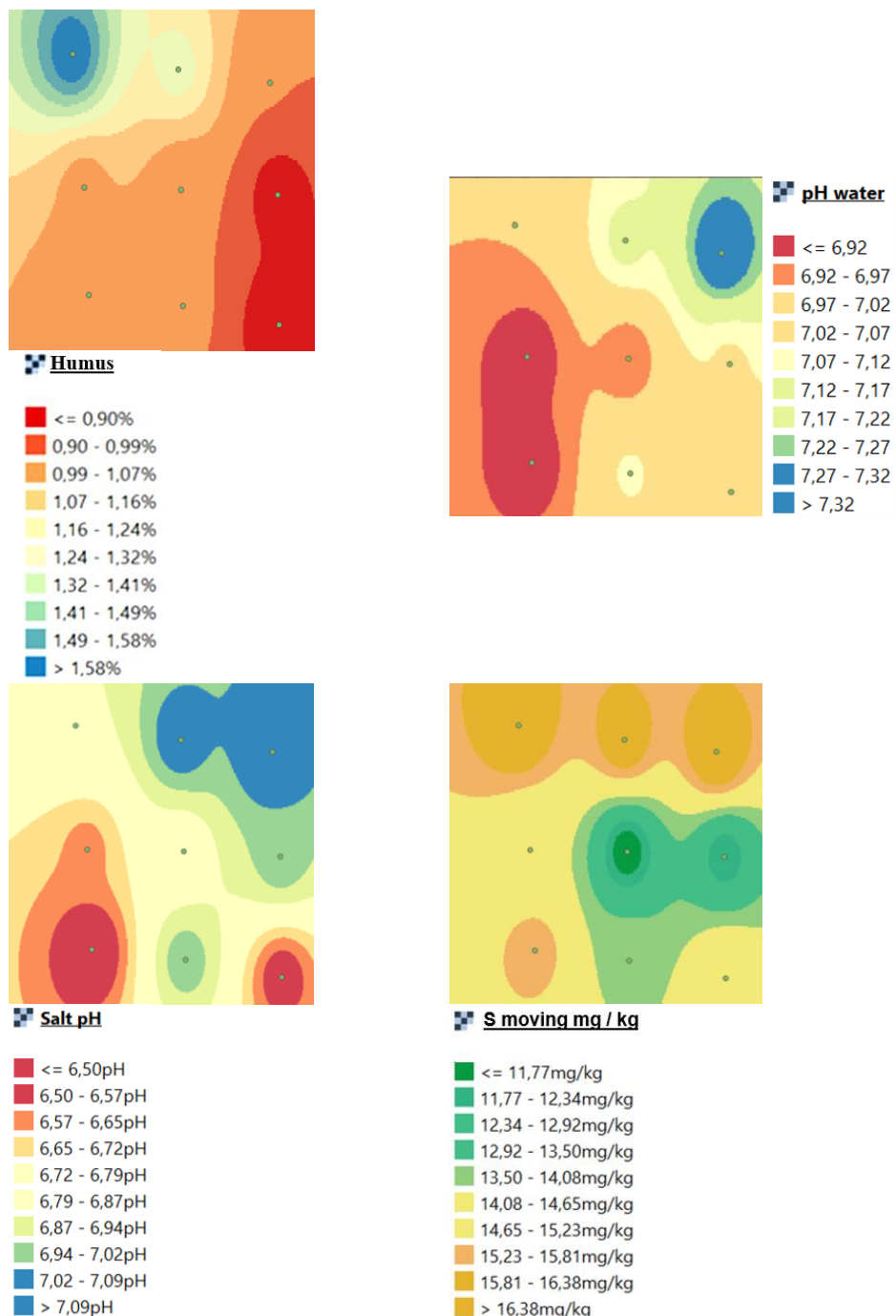
Soil sample No.	Contents								
	Humus, %	pH, Aqueous	S Mobile, mg/kg	N total, mg/kg	N total, mg/100 g of soil	K <sub>2</sub> O, mg/kg	K <sub>2</sub> O, mg/100 g of soil	P <sub>2</sub> O <sub>5</sub> , mg/kg	P <sub>2</sub> O <sub>5</sub> , mg/100 g of soil
(polygon 1)									
A1	4,39	8,04	27,92	2604	260,4	384	38,4	62,03	6,20
A2	4,41	7,93	28,24	2240	224	362	36,2	59,17	5,92
A3	4,27	7,85	31,55	2156	215,6	354	35,4	56,30	5,63
A4	4,58	6,68	28,64	2604	260,4	378	37,8	61,08	6,11
A5	4,72	7,05	31,58	2800	280	366	36,6	54,40	5,44
A6	4,37	6,95	32,97	2296	229,6	390	39,0	59,17	5,92
A7	5,32	7,16	31,5	3108	310,8	396	39,6	62,98	6,30
A8	4,06	8,02	33,21	2324	232,4	362	36,2	66,80	6,68
A9	4,19	8,01	33,53	2464	246,4	374	37,4	66,80	6,68
(polygon 2)									
A1	3,50	7,51	25,38	2100	210,0	386	38,64	125,1	12,50
A2	3,85	6,28	29,34	2100	210,0	390	39,09	93,4	9,34
A3	3,96	6,62	19,17	2380	238,0	425	42,50	102,2	10,22
A4	5,50	5,59	22,79	2744	274,4	490	49,09	86,3	8,63
A5	4,81	6,84	32,21	2772	277,2	384	38,41	70,5	7,05
A6	4,00	6,56	30,33	2044	204,4	406	40,68	107,5	10,75
A7	4,49	6,71	28,08	2520	252,0	445	44,55	100,4	10,04
A8	3,85	6,21	26,64	2268	226,8	436	43,64	105,7	10,57
A9	3,78	6,30	27,42	2100	210,0	393	39,32	75,8	7,58
(polygon 3)									
A1	1,35	7,48	16,35	924	92,40	269	26,91	90,1	9,01
A2	1,1	7,19	14,82	728	72,80	290	29,09	91,6	9,16
A3	0,86	6,95	12,72	560	56,00	261	26,18	91,6	9,16
A4	0,99	6,71	11,7	336	33,60	300	30,00	53,4	5,34
A5	0,91	7,04	11,96	560	56,00	274	27,45	90,1	9,01
A6	0,78	7,03	11,64	588	58,80	256	25,64	88,6	8,86
A7	0,96	7,02	9,6	672	67,20	296	29,64	91,6	9,16
A8	0,78	7,17	8,15	336	33,60	281	28,18	76,3	7,63
A9	1,42	6,89	8,85	588	58,80	300	30,00	94,7	9,47

The amount of available phosphorus (P<sub>2</sub>O<sub>5</sub>) ranged from 70.47 to 125.09 mg/kg, while the amount of available potassium (K<sub>2</sub>O) varied between 384.09 and 490.91 mg/kg. These values indicate that the studied soils are highly supplied with potassium and moderately supplied with phosphorus. Additionally, the studied sites exhibited an uneven spatial distribution of mobile nutrients, highlighting the need for site-specific fertilizer application [Petukhov et al., 2021].

Similar studies conducted on Polygon 3 revealed that the humus content in the soil ranged from 0.78 to 1.49 %, indicating that the nutrient supply is insufficient for obtaining 1 ton of the main product through agricultural management [Gurov et al., 2019].

Researchers recommend using “Nitroammophoska” as a mineral fertilizer when determining fertilizer application rates and estimating the projected yield of spring barley under irrigated conditions. Its physical mass can reach up to 400 kg, while in terms of active ingredients per 100 kg of fertilizer; it contains 12 % nitrogen, 12 % phosphorus, and 12 % potassium, along with up to 6 % sulfur, which fully aligns with the application rates for spring barley under irrigation.

A soil map was created using QGIS software based on the agrochemical analysis of soil from the three experimental polygons, and a fragment of the maps for Polygon 1 is presented in this article (Fig. 4).



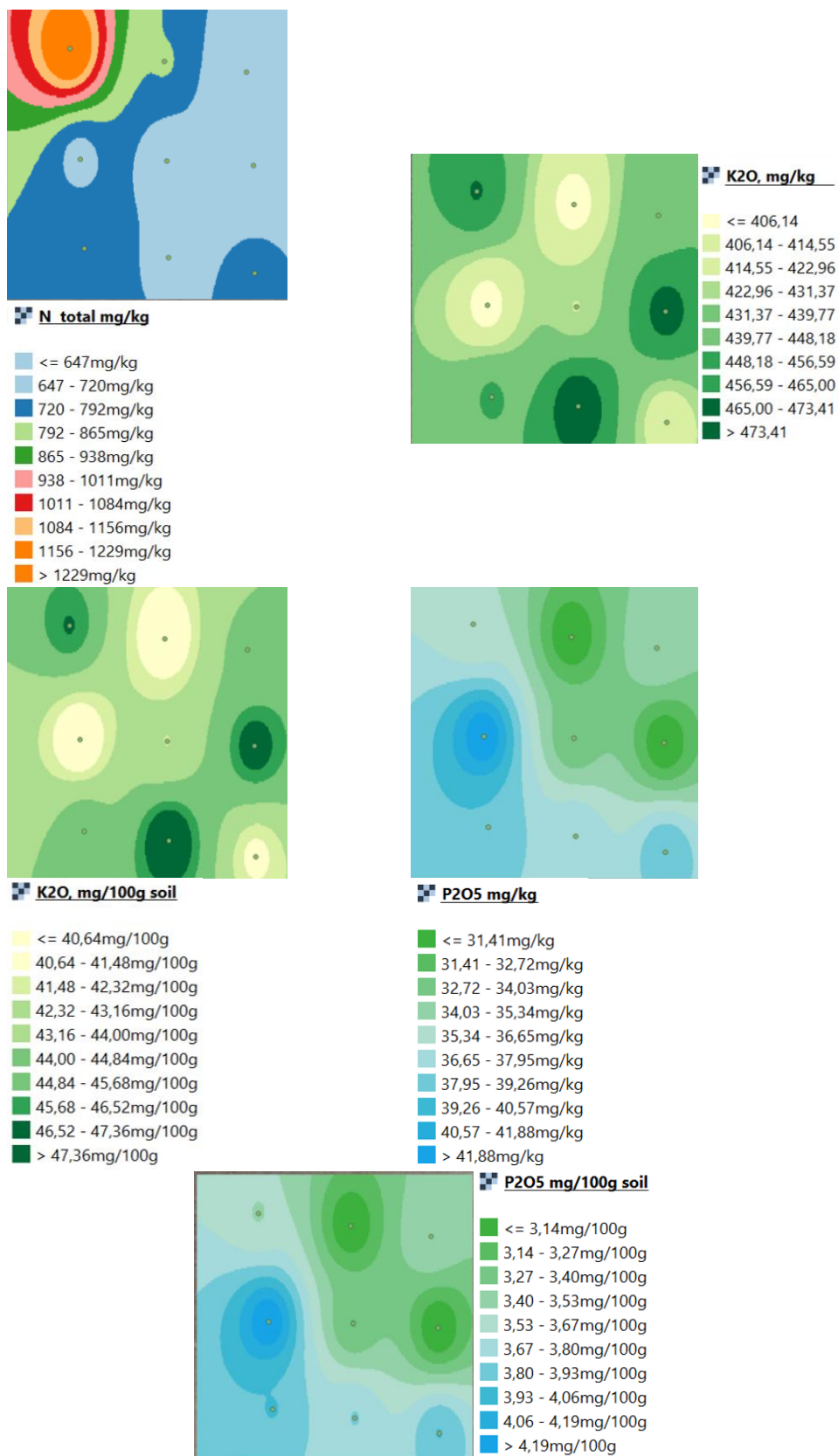


Fig. 4. Cartogram of the distribution of agrochemical indicators in the soil

For non-irrigated “rainfed” lands, researchers apply different criteria to estimate the projected yield of spring barley. Specifically, when the expected yield under irrigated conditions is 20 c/ha, the required nutrient amounts amount to 48 kg of nitrogen, 48 kg of phosphorus, and 48 kg of potassium in terms of active ingredients. Based on the study results, the actual obtained yield of spring barley was 9 c/ha.

The peculiarity of using information technologies in agriculture is that almost all the data utilized have a spatial (geographical) connection [Zolkin et al., 2021]. The processing of such data is performed exclusively through specialized software designed to work with spatial information, among which Geographic Information Systems “GIS” play a crucial role.

Various vegetation indices serve to assess the productivity of crop plants [Kurbanov et al., 2020]. According to the research of scientists, the following types of indices are applicable to determine the condition of crop plants: GRRI, GBRI, RBRI, NDYI, RVI, NDVI, MTVI, EVI, MSAVI, and TCARI. In the process of identifying and analyzing vegetation indices, data obtained from Landsat-8–9 OLI remote sensing and DJI Phantom 4 RTK UAV systems are utilized [Ganie, Nusrath, 2016; Pan et al., 2023]. The data is obtained over a specific period, and a comparative analysis between them is conducted. This approach enables the assessment of vegetation conditions, prediction of crop yields, and planning of agrotechnical measures.

Among the indices mentioned above, the NDVI “Normalized Difference Vegetation Index” is widely used to determine the overall condition of plants, the density of green biomass, and photosynthetic activity. In our study, we performed the differentiation using the NDVI index [Huang et al., 2021]. We calculate this index using the following formula (1):

$$\text{NDVI} = (\text{NIR} - \text{R}) / (\text{NIR} + \text{R}) \quad (1),$$

where NIR refers to the Near Infrared spectral band, and R refers to the Red spectral band.

In figures 5a, 6a, and 7a the NDVI values, calculated based on the processing of Landsat-8–9 OLI/TIRS C2 L2 satellite images obtained from the EO Browser open-access platform, are presented for different vegetation periods.

In addition, we present the NDVI values obtained from images taken by the DJI Phantom 4 RTK multispectral unmanned aerial vehicle at an altitude of 100 m during the same periods as those from the satellite (Fig. 5b, 6b, 7b).

The spatial resolution of the images obtained through the UAV is 5.4 cm (focal length — 5.74 mm, speed — 7.5 m/s, horizontal overlap — 90 %, longitudinal overlap — 80 %).

The results of the study indicate that, depending on the data source, the average NDVI value for May for the first polygon was as follows: 0.16 based on satellite images (Fig. 5a) and 0.20 based on UAV data (Fig. 5b). Based on the analysis of UAV and satellite image data, the Pearson correlation coefficient was calculated as  $r = 0.98$ , which demonstrates a high correlation.

Further, for the second polygon in May, the average “NDVI” value was as follows: 0.20 based on satellite images (Fig. 6a) and 0.32 based on “UAV” data (Fig. 6b). Based on the analysis of UAV and satellite image data, the Pearson correlation coefficient was calculated as  $r = 0.87$ , which also demonstrates a high correlation.

To ensure consistency and improve visual interpretation, all NDVI maps (Figures 5b, 6b, 7b, and 8) were standardized using a unified color legend ranging from 0.0 (low vegetation index) to 1.0 (high vegetation index). Green tones indicate areas of dense and healthy vegetation, while yellow to red tones represent sparse or stressed vegetation.

In addition, the field boundaries for Polygons 1–3 were delineated and overlaid on each NDVI map to clearly indicate the spatial extent of each experimental area. This allows for precise visual correlation between NDVI changes and specific fertilized or control zones within the fields.

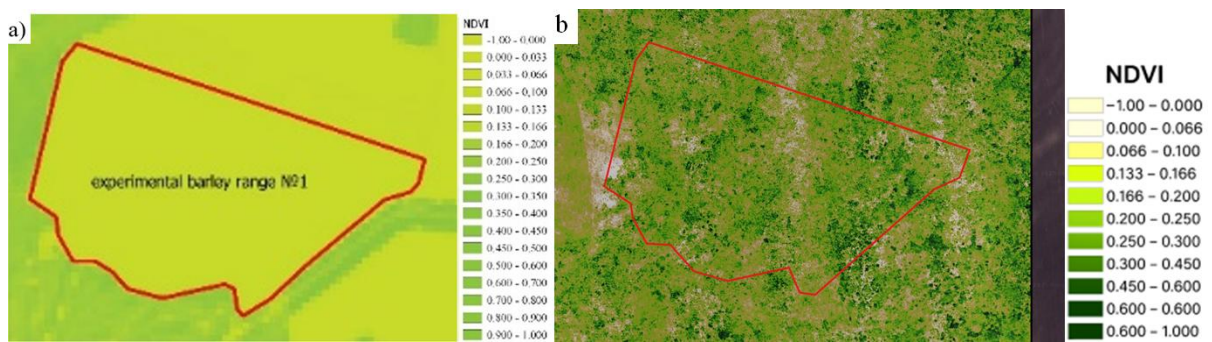


Fig. 5. NDVI values calculated based on: a) satellite data; b) UAV data (polygon 1, 14.05.22)

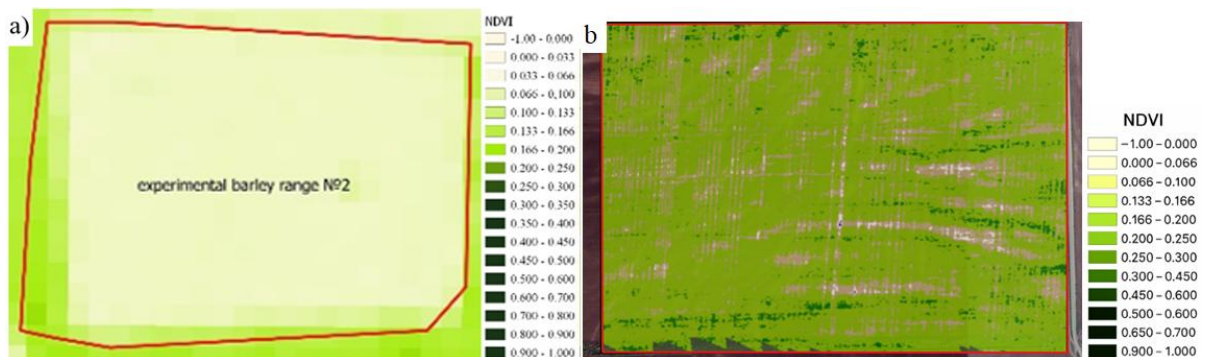


Fig. 6. NDVI values for polygon 2 on 25.05.22: a) processed NDVI image based on satellite data; b) processed NDVI image based on UAV data

And, for the third polygon in May, the average NDVI value was as follows: 0.27 based on satellite images (Fig. 7a) and 0.29 based on UAV data (Fig. 7b). Based on the analysis of “UAV” and satellite image data “RS”, the Pearson correlation coefficient was calculated as  $r = 0.98$  (high correlation).

Based on the study results, differential fertilizer doses were determined and applied to field polygons with macronutrient deficiencies [Michaud et al., 2020; Shiawakoti et al., 2020] (Table 2). Fertilizer rates were calculated by integrating NDVI data from UAV imagery with spatial agrochemical indicators derived from soil samples (0–30 cm depth). The analysis focused on nitrogen (N), phosphorus ( $P_2O_5$ ), and potassium ( $K_2O$ ) content.

Agrochemical maps were created in QGIS using interpolated laboratory results, and NDVI maps were generated from multispectral UAV imagery captured during early barley growth. Overlaying these datasets enabled the identification of underperforming zones with  $NDVI < 0.3$  and nitrogen  $< 2300 \text{ mg/kg}$ . These zones received a uniform dose of 12 kg/ha, of N-P-K (Nitroammophoska), while control plots in the same fields remained unfertilized.

For example, in Polygon 1, several 5-ha plots with low NDVI and nitrogen levels were fertilized. The same approach was applied in Polygons 2–3, adjusted for local nutrient profiles. UAV and GIS integration ensured precise, site-specific application.

A 15–20 % increase in NDVI was observed in treated plots compared to controls, based on monthly UAV monitoring. NDVI values rose from ~0.20 to 0.55–0.64 in fertilized plots, while control plots remained at ~0.19–0.22. This improvement, strongly correlated with crop biomass in prior studies, served as a proxy for yield increase. The consistent pattern across all polygons supports the effectiveness of differential fertilization guided by UAV and GIS technologies.

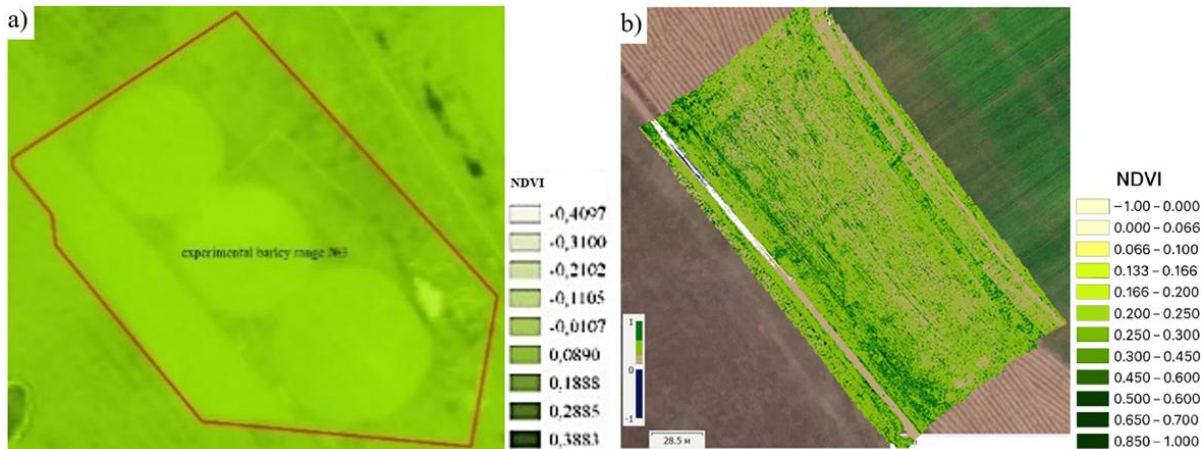


Fig. 7. NDVI values for polygon 3 on 25.05.2022: a) processed NDVI image based on satellite data; b) processed NDVI image based on UAV data

Table 2. Effect of mineral fertilizers on spring barley yield under conditions of high soil phosphorus and potassium availability

Variant	Fertilizer composition, active substance (kg/ha)	Irrigated yield (c/ha)	Rainfed yield (c/ha)
$N_0P_0K_0$	Control	6,0	3,5
Nitroammophoska, $N_{12}P_{12}K_{12}$	12 kg/ha N.P.K	9,0	3,5

To evaluate fertilizer effectiveness [Tucher et al., 2018], Landsat-8–9 OLI satellite imagery was analyzed one month after application during the spring barley growing season (Fig. 8a–8c). In Polygon 1 (Fig. 8a), NDVI increased from 0.13 to 0.21 compared to the initial stage, with post-treatment values ranging from 0.55 to 0.64, indicating enhanced vegetation vigor.

Initially, NDVI values in both treated and control plots were similar. However, UAV-based monitoring [Grados, Schrevens, 2023] showed that in treated areas (points 1, 2, 4, 5, 7, 8), NDVI rose to 0.55–0.64, while control areas remained around 0.19, confirming the treatment effect.

In Polygon 2 (Fig. 8b), NDVI initially ranged from 0.10 to 0.13. One month after applying differentiated fertilizer doses, values increased to 0.52. This improvement under chernozem soil conditions indicates favorable growth dynamics and high yield potential.

In Polygon 3, during the first vegetation period, the NDVI growth intensity of spring barley ranged from 0.08 to 0.18. After adjusting the composition of the applied fertilizers (macroelements) based on the coordinates of the determined soil sample, an increase in NDVI growth intensity from 0.18 to 0.62 was observed over a 25-day growth period (Fig. 8c).



Fig. 8. NDVI values derived from Landsat-8–9 OLI satellite imagery one month after fertilizer application: a) polygon No. 1; b) polygon No. 2; c) polygon No. 3

During the study conducted on Polygons 1–3, intra-field variability during the vegetation period appeared in nearly all agricultural fields. This, in turn, provides evidence that the initial results in developing the fundamental formula for spring barley cultivation emerged on sandy-chestnut soils and non-irrigated arable lands.

The results demonstrated a significant correlation ( $r = 0.98$ ) between NDVI data obtained from satellites and data collected using UAVs [Fan, 2023]. The analysis showed that UAVs enable the rapid assessment of crop conditions and the adjustment of fertilization strategies. On the experimental plots, NDVI increased by 15–20 % after fertilizer application. In this study, the NDVI (Normalized Difference Vegetation Index) served as the primary indicator of crop productivity. Higher NDVI values were interpreted as indicators of healthier, denser green biomass, and thus greater expected yield. The 15–20 % increase in NDVI was therefore used as a proxy for yield improvement following fertilization.

While Fig. 5–7 present NDVI distributions within individual fields using UAV data, Fig. 8 summarizes the treatment effect across the three polygons using satellite-based NDVI measurements (Landsat-8–9 OLI). To ensure consistency in interpretation, all NDVI maps (including Fig. 8) were harmonized to use a standardized color legend (range: 0.0 to 1.0).

Field boundaries and treatment/control zones were also delineated to facilitate visual comparison. Although the data sources differ (UAV vs. satellite), the comparative NDVI dynamics clearly demonstrate the effectiveness of site-specific fertilization methods applied in this study.

## CONCLUSIONS

This study demonstrated the effectiveness of integrating Unmanned Aerial Vehicles (UAVs), remote sensing (RS), and Geographic Information Systems (GIS) technologies for assessing agricultural productivity and optimizing fertilizer application in various soil-climatic zones of Kazakhstan. By combining high-resolution UAV multispectral imagery with laboratory-based agrochemical soil data, researchers were able to generate spatially explicit fertilization schemes tailored to field-specific conditions.

The NDVI index served as the primary indicator for evaluating crop health and estimating yield potential. Monthly UAV monitoring revealed a consistent 15–20 % increase in NDVI values in fertilized plots compared to control plots without fertilization. This increase was used as a proxy for yield improvement and confirmed the impact of site-specific nutrient management.

Unlike prior studies relying solely on satellite imagery, this research introduced a layered spatial analysis by linking NDVI maps directly to interpolated agrochemical indicators in QGIS. This methodology enabled a localized understanding of nutrient variability and informed precise fertilizer allocation at the sub-field level.

The scientific novelty of this approach lies in its operational integration of UAV and GIS tools for differential fertilization across diverse agroecological settings. Though the experiments were conducted on three fields, the techniques and workflows demonstrated here are scalable and transferable to other regions with similar environmental conditions.

Overall, the results highlight the strong potential of precision agriculture to enhance productivity, reduce excessive fertilizer use, and support sustainable land management. The adoption of these digital technologies presents a viable pathway for modernizing Kazakhstan's agricultural sector while minimizing its environmental footprint.

## REFERENCES

Abedzhanova A. S., Dzhaxylykov A. F., Rasskazov P. A., Apshikur B., Islyam G. Automated System for Optimizing the Movement of Urban Passenger Transport Using GIS. The International Archives of the Photogrammetry, Remote Sensing and Spatial Information Sciences, 2023. V. XLVIII-5/W2-2023. P. 1–8. DOI: 10.5194/ISPRS-Archives-XLVIII-5-W2-2023-1-2023.

*Apshikur B., Alimkulov M. A., Kapasov A. K., Toleubekyzy I. T.* Innovative Technology for Assessing the Degradation of the Earth by Sand Desertification of Soils with Specialized Processing of Space Materials. InterCarto. InterGIS. Moscow: Lomonosov Moscow State University, Faculty of Geography, 2024. V. 30. Part 2. P. 223–235 (in Russian). DOI: 10.35595/2414-9179-2024-2-30-223-235.

*Apshikur B., Kurmangaliyev T. B., Goltsev A. G., Alimkulov M. M., Kapasov A. K.* The Method of Multi-Criteria Analysis for Determining the Flood-Hazardous Area and the Development of Protective Structures. The International Archives of Photogrammetry, Remote Sensing and Spatial Information Sciences, 2023. V. XLVIII-5/W2-2023. P. 9–17. DOI: 10.5194/ISPRS-archives-XLVIII-5-W2-2023-9-2023.

*Apshikur B., Maksimov V. A., Toleubekyzy I. T., Alimkulov M. M.* Current Assessment of Atmospheric Pollution by Industrial Enterprises in Ust-Kamenogorsk Based on GIS Technologies. InterCarto. InterGIS. Moscow: Lomonosov Moscow State University, Faculty of Geography, 2024. V. 30. Part 2. P. 469–481 (in Russian). DOI: 10.35595/2414-9179-2024-2-30-469-481.

*Apshikur B., Rakhymerdina M., Levin E., Toguzova M., Daumova G., Assylkhanova Zh., Kapasov A., Kolpakova V.* Integrated Research of the Transboundary Yertis River Using Modern Monitoring Methods and Bathymetric Survey. ES Energy & Environment, 2025. V. 27. P. 1362. DOI: 10.30919/esee1362.

*Asangaliyev E. A., Apshikur B., Lutay S. S., Assylkhanova Z. A.* Spatial Analysis and Mapping of Potential Wildfires from Landsat Satellite Data. InterCarto. InterGIS. Moscow: Lomonosov Moscow State University, Faculty of Geography, 2024. V. 30. Part 1. P. 476–490 (in Russian). DOI: 10.35595/2414-9179-2024-1-30-476-490.

*Bakaeva N. P., Vasiliev A. S., Zakharova O. A.* Efficiency of Herbicide Treatment Against Weed Vegetation in Intensive Technology of Spring Barley Cultivation. Bulletin of Samara State Agricultural Academy, 2024. V. 9. No. 1. P. 18–26. DOI: 10.55170/1997-3225-2024-9-1-18-26.

*Beluhova-Uzunova R. P., Dunchev D. M.* Precision Farming — Concepts and Perspectives. Problems of Agricultural Economics, 2019. V. 360. No. 3. P. 142–155. DOI: 10.30858/zer/112132.

*Boiarskii B., Hasegawa H.* Comparison of NDVI and NDRE Indices to Detect Differences in Vegetation and Chlorophyll Content. Journal of Mechanics of Continua and Mathematical Sciences, 2019. Special Iss. No. 4. P. 20–29. DOI: 10.26782/jmcms.spl.4/2019.11.00003.

*Cao Zh., Kooistra L., Wang W., Guo L., Valente J.* Real-Time Object Detection Based on UAV Remote Sensing: A Systematic Literature Review. Drones, 2023. V. 7. No. 10. P. 620–629. DOI: 10.3390/drones7100620.

*Deikun V., Zhuk D., Machok Y.* Overview of Application Methods and Application Efficiency Mineral Fertilizers. National Interagency Scientific and Technical Collection of Works. Design, Production and Exploitation of Agricultural Machines, 2022. P. 41–47. DOI: 10.32515/2414-3820.2022.52.41-47.

*Eranova M., Simakina A., Yakubailik O.* Smart Analysis of Agricultural Land Use with NDVI at Kuraginskoye Agricultural Experimental Production Facility. IOP Conference Series: Earth and Environmental Science, 2021. V. 677. P. 032105. DOI: 10.1088/1755-1315/677/3/032105.

*Fan D.* Research on the Establishment of NDVI Long-Term Data Set Based on a Novel Method. Scientific Reports, 2023. V. 13. No. 1. P. 337–347. DOI: 10.1038/s41598-023-36939-y.

*Ganie M. A., Nusrath A.* Determining the Vegetation Indices (NDVI) from Landsat-8 Satellite Data. International Journal of Advanced Research, 2016. V. 4. No. 8. P. 1459–1463. DOI: 10.21474/IJAR01/1348.

*Gonçalves J., Ferraz G., Reynaldo É., Marin D., Ferra P., Pérez-Ruiz M., Rossi G., Vieri M., Sarri D.* Comparative Analysis of Soil-Sampling Methods Used in Precision Agriculture. Journal of Agricultural Engineering, 2021. V. 52. No. 1. P. 1–12. DOI: 10.4081/jae.2021.1117.

*Górski R., Robert R., Niewiadomska A., Wolna-Maruwka A., Plaza A.* Innovative Spring Barley Cultivation Technology Based on the Use of Microbial Products Together with Living Mulch in Organic Farming. Agronomy, 2023. V. 13. Iss. 7. P. 1914. DOI: 10.3390/agronomy13071914.

*Grados D., Schrevens E.* Cassava NDVI Analysis: A Nonlinear Mixed Model Approach Based on UAV-Imagery. Journal of Photogrammetry, Remote Sensing and Geoinformation Science, 2020. V. 88. No. 3. P. 337–347. DOI: 10.1007/s41064-020-00116-x.

*Gurov A., Shirokova V., Khutorova A., Yurova Yu.* Features of Remote Determination of Humus Content in Arable Soils. Advances in Engineering Research VIII All-Russian Science and Technology Conference, 2019. V. 182. No. 3. P. 138–144. DOI: 10.2991/ciggg-18.2019.25.

*Hoffland E., Kuyper Th., Coman R., Creamer R.* Eco-Functionality of Organic Matter in Soils. Plant Soil, 2020. V. 455. P. 1–22. DOI: 10.1007/s11104-020-04651-9.

*Huang Y., Reddy K. N., Fletcher R. S., Pennington D.* UAV Low-Altitude Remote Sensing for Precision Weed Management. Weed Technology, 2018. V. 32. No. 1. P. 2–6. DOI: 10.1017/wet.2017.89.

*Huang Sh., Tang L., Hupy J., Wang Y., Shao G.* A Commentary Review on the Use of Normalized Difference Vegetation Index (NDVI) in the Era of Popular Remote Sensing. Journal of Forestry Research, 2021. V. 32. P. 1–6. DOI: 10.1007/s11676-020-01155-1.

*Huuskonen J., Oksanen T.* Soil Sampling with Drones and Augmented Reality in Precision Agriculture. Computers and Electronics in Agriculture, 2018. V. 154. P. 25–35. DOI: 10.1016/j.compag.2018.08.039.

*Jindo K., Kozan O., Iseki K., Maestrini B., Van Evert F., Yilma W., Arai E., Shimabukuro Y., Sawada Y., Kempenaar C.* Potential Utilization of Satellite Remote Sensing for Field-Based Agricultural Studies. Chemical and Biological Technologies in Agriculture, 2021. V. 8. No. 58. DOI: 10.1186/s40538-021-00253-4.

*Korchagin A., Mazirov M., Shchukin I., Shchukina W., Petrosyan R., Shilov P.* Differentiated Fertilization in the System of Precision Farming on the Complex of Gray Forest Soils in Vladimir Opolye. IOP Conference Series: Earth and Environmental Science, 2021. V. 852. P. 012051. DOI: 10.1088/1755-1315/852/1/012051.

*Kulyasov N., Novik N., Klyukin N., Charyyarova G.* Precision Agriculture in the Russian Federation: Problems and Directions in Development. IOP Conference, Series: Earth and Environmental Science, 2020. V. 548. P. 022090. DOI: 10.1088/1755-1315/548/2/022090.

*Kurbanov R. K., Zakharova N. I.* Application of Vegetation Indexes to Assess the Condition of Crops. Agricultural Machinery and Technologies, 2020. V. 14. No. 4. P. 4–11 (in Russian). DOI: 10.22314/2073-7599-2020-14-4-4-11.

*Lebrini Y., Boudhar A., Htitiou A., Hadria R., Lionboui H., Bounoua L., Benabdellahab T.* Remote Monitoring of Agricultural Systems Using NDVI Time Series and Machine Learning

Methods: A Tool for an Adaptive Agricultural Policy. *Arabian Journal of Geosciences*, 2020. V. 13. P. 796. DOI: 10.1007/s12517-020-05789-7.

*Lukin S. V.* Dynamics of the Agrochemical Fertility Parameters of Arable Soils in the Southwestern Region of Central Chernozemic Zone of Russia. *Eurasian Soil Science*, 2017. V. 50. P. 1323–1331. DOI: 10.1134/S1064229317110096.

*Michaud A., Cambier Ph., Sappin-Didier V., Deltreil V., Mercier V., Rampon J.-N., Houot S.* Mass Balance and Long-Term Soil Accumulation of Trace Elements in Arable Crop Systems Amended with Urban Composts or Cattle Manure During 17 Years. *Environmental Science and Pollution Research*, 2020. V. 27. P. 5367–5386. DOI: 10.1007/s11356-019-07166-8.

*Muraru S., Muraru V., Condruz P., Ionel C., Sfiru R.* Considerations on the Importance of the Main Chemical Properties of the Soil in Agrochemical Studies. *E3S Web of Conferences*, 2021. V. 286. P. 03019. P. 1–9. DOI: 10.1051/e3sconf/202128603019.

*Pan W., Wang X., Sun Y., Wang J., Li Y., Li Sh.* Karst Vegetation Coverage Detection Using UAV Multispectral Vegetation Indices and Machine Learning Algorithm. *Plant Methods*, 2023. V. 19. No. 7. P. 1–16. DOI: 10.1186/s13007-023-00982-7.

*Petukhov D., Ivanov A., Bondarenko E., Trubnikov A., Semizorov S.* The Efficiency of the Differentiated Application of Mineral Fertilizers in the Production Technology of Winter Wheat Cultivation. *IOP Conference Series, Earth and Environmental Science*, 2021. V. 723. P. 032042. P. 1–5. DOI: 10.1088/1755-1315/723/3/032042.

*Phang S. K., Chiang T. H. A., Happonen A., Chang M. M. L.* From Satellite to UAV-Based Remote Sensing: A Review on Precision Agriculture. *IEEE Access*, 2023. V. 11. P. 127057–127076. DOI: 10.1109/ACCESS.2023.3330886.

*Ryzhkov S. O., Portnov V. S., Huangan N. Kh., Rakhimov M., Khmyrova E. N.* Research into Stability of Tailings Storage at Vostochnaya Coal Processing Plant (Central Kazakhstan) to Assess its Safe Conservation and Abandonment. *Ugol*, 2021. No. 12-2021/1149/. P. 57–62 (in Russian). DOI: 10.18796/0041-5790-2021-12-57-62.

*Sadenova M. A., Beisekenov N. A., Apshikur B., Khrapov S. S., Kapasov A. K., Mamysheva A. M., Klemeš J. J.* Modelling of Alfalfa Yield Forecasting Based on Earth Remote Sensing (ERS) Data and Remote Sensing Methods. *Chemical Engineering Transactions*, 2022. V. 94. P. 697–702. DOI: 10.3303/CET2294116.

*Shiwakoti S., Zheljazkov V. D., Gollany H. T., Kleber M., Xing B., Astatkie T.* Macronutrient in Soils and Wheat from Long-Term Agroexperiments Reflects Variations in Residue and Fertilizer Inputs. *Scientific Reports*, 2020. V. 10. P. 3263. DOI: 10.1038/s41598-020-60164-6.

*Surinov A. V.* Agro-Ecological Assessment of the Condition of Arable Soils of the CCR. *IOP, Conference Series*, 2023. V. 1206. P. 012011. P. 1–8. DOI: 10.1088/1755-1315/1206/1/012011.

*Toguzova M. M., Rakhymberdina M. Y., Kulenova N. A., Shaimardanov Z. K., Assylkhanova Zh. A., Apshikur B., Beisekenov N. A.* Analysis of Process Modeling in Modern Software Program to Support “Smart” Agriculture. *Chemical Engineering Transactions*, 2022. V. 94. P. 871–876. DOI: 10.3303/CET2294145.

*Tucher Von S., Hörndl D., Schmidhalter U.* Interaction of Soil pH and Phosphorus Efficacy: Long-Term Effects of P Fertilizer and Lime Applications on Wheat, Barley, and Sugar Beet. *Ambio*, 2018. V. 47 (Suppl. 1). P. 41–49. DOI: 10.1007/s13280-017-0970-2.

*Vlasenko N. G., Korotkikh N. A., Myakisheva O. A.* Response of Spring Barley Subspecies to Herbicides. Russian Agricultural Sciences, 2011. V. 37. P. 465–468 (in Russian) DOI: 10.3103/S1068367411060206.

*Yang Z., Bai Z., Qin Z.* A New Soil Sampling Design Method Using Multi-Temporal and Spatial Data Fusion. Environmental Science and Pollution Research International, 2022. V. 29. P. 21023–21033. DOI: 10.1007/s11356-021-17200-3.

*Yapiyev V., Gilman Ch., Kabdullayeva T., Suleimenova A., Shagadatova A., Duisembay A., Naizabekov S., Mussurova S., Sydykova K., Raimkulov I., Kabimoldayev I., Abdrahmanova A., Omarkulova S., Nurmukhambetov D., Kudarova A., Malgazhdar D., Schönbach Ch., Inglezakis V.* Top Soil Physical and Chemical Properties in Kazakhstan Across a North-South Gradient. Scientific Data, 2018. V. 5. P. 180242. DOI: 10.1038/sdata.2018.242.

*Zolkin A., Shavanov M., Hmizova N.* Features of the Use of Information Technologies in Agriculture. IOP Conference Series: Earth and Environmental Science, 2021. V. 677. P. 032091. P. 1–5. DOI: 10.1088/1755-1315/677/3/032091.

---